

Molecular spin-orbit excitations in the $J_{\text{eff}}=\frac{1}{2}$ frustrated spinel GeCo_2O_4

K. Tomiyasu,^{1,*} M. K. Crawford,² D. T. Adroja,³ P. Manuel,³ A. Tominaga,⁴ S. Hara,⁴ H. Sato,⁴ T. Watanabe,⁵ S. I. Ikeda,⁶ J. W. Lynn,⁷ K. Iwasa,¹ and K. Yamada⁸

¹*Department of Physics, Tohoku University, Aoba, Sendai 980-8578, Japan*

²*Central Research and Development Department, DuPont, Wilmington, Delaware 19880, USA*

³*ISIS Facility, Rutherford Appleton Laboratory, Chilton, Didcot, OX11 0QX, UK*

⁴*Department of Physics, Chuo University, Bunkyo, Tokyo 101-8324, Japan*

⁵*Department of Physics, CST, Nihon University, Chiyoda, Tokyo 101-8308, Japan*

⁶*Nanoelectronics Research Institute, National Institute of AIST, Tsukuba 305-8568, Japan*

⁷*NIST Center for Neutron Research, Gaithersburg, Maryland 20899, USA*

⁸*WPI AIMR, Tohoku University, Aoba, Sendai 980-8577, Japan*

(Received 21 February 2011; revised manuscript received 8 May 2011; published 2 August 2011)

We describe powder and single-crystal inelastic neutron scattering experiments on a spinel-type antiferromagnet GeCo_2O_4 , represented by an effective total angular momentum $J_{\text{eff}} = 1/2$. Several types of nondispersive short-range magnetic excitations were discovered. The scattering intensity maps in \mathbf{Q} space are well reproduced by dynamical structure factor analyses using molecular model Hamiltonians. The results of analyses suggest that the molecular excitations below T_N arise from molecular ground states, one of which consists of antiferromagnetically coupled ferromagnetic subunits. The quasielastic excitations above T_N are interpreted as its precursor. A combination of frustration and $J_{\text{eff}} = 1/2$ might induce these quantum phenomena.

DOI: [10.1103/PhysRevB.84.054405](https://doi.org/10.1103/PhysRevB.84.054405)

PACS number(s): 75.30.-m, 75.40.Gb, 75.50.Xx, 78.70.Nx

I. INTRODUCTION

Since its initial proposal,¹⁻³ the concept of geometrical spin frustration has been intensively studied. Geometrical frustration has been shown to give rise to novel forms of spin-liquid-like fluctuations in a paramagnetic phase, such as spin molecules, spin ices, and spin vortices.⁴⁻⁹ Recently, dynamical spin molecules were discovered as nondispersive excitation modes within a magnetically ordered phase, where frustration was assumed to be relieved by a lattice deformation.¹⁰

Meanwhile, it was demonstrated that an effective total angular momentum $J_{\text{eff}} = 1/2$, generated by a spin-orbit coupling (SOC), provides a new playground for correlated electrons. For example, a Mott instability with spin-orbit integrated narrow band was confirmed in Sr_2IrO_4 , and a quantum spin-hall effect at room temperature was theoretically predicted for Na_2IrO_3 .¹¹⁻¹³ These iridates possess Ir^{4+} with low-spin (t_{2g})⁵ configuration, of which the ground states are described by $J_{\text{eff}} = 1/2$ with unquenched orbital angular momentum ($L = 1$). The $L = 1$ states are related to t_{2g} triplets (xy, yz, zx): $|L^z = \pm 1\rangle = (|yz\rangle \pm i|zx\rangle)/\sqrt{2}$ and $|L^z = 0\rangle = |xy\rangle$. The value of $1/2$ and the complex orbitals of J_{eff} are expected to enhance the quantum nature accompanied with orbital degree of freedom.¹³

Then, an interest in the combination of frustration and $J_{\text{eff}} = 1/2$ will naturally arise. In fact, there are reports of Ir^{4+} systems, e.g., a face-centered cubic system K_2IrCl_6 forming a magnetic complex IrCl_6 with a remarkably mixed orbital, a hyperkagome system $\text{Na}_4\text{Ir}_3\text{O}_8$ with a quantum spin liquid, and pyrochlore systems $\text{Ln}_2\text{Ir}_2\text{O}_7$ ($\text{Ln}=\text{Nd, Sm, Eu}$) with metal-insulator transition.¹⁴⁻¹⁷ However, an extremely strong neutron absorption of Ir nuclei (~ 425 b for thermal neutrons)¹⁸ and the lack of large single crystals hamper the successful inelastic neutron scattering experiments, a prime tool for the study of magnetic frustration.

The spinel-type antiferromagnet GeCo_2O_4 is a promising candidate with frustration and $J_{\text{eff}} = 1/2$. In this material, well-known SOC-active Co^{2+} ions octahedrally surrounded by anions form a lattice of corner-sharing tetrahedra, which is geometrically frustrated, and Ge^{4+} ions are nonmagnetic. Figure 1(a) shows the energy-level schemes of a single-ion state of Co^{2+} (d^7). The crystal field and SOC yield $J_{\text{eff}} = 1/2, 3/2,$ and $5/2$ states with $L = 1$ and high-spin $S = 3/2$.¹⁹⁻²² Antiferromagnetic order with propagation vector $\mathbf{q}_m = (1/2, 1/2, 1/2)$ and a tiny tetragonal lattice deformation ($c/a \simeq 1.001$) simultaneously occur at $T_N \simeq 21$ K, which is suppressed compared to the Curie-Weiss temperature $\theta_W \simeq 81$ K.²³⁻²⁶ Spin-liquid-like fluctuations above T_N (quasielastic mode) and a nondispersive magnetic excitation mode below T_N (4-meV mode) were also found by powder inelastic neutron scattering.²¹

In this paper, we comprehensively study magnetic excitations above and below T_N in GeCo_2O_4 in wide momentum (\mathbf{Q}) and energy (E) ranges by powder and single-crystal inelastic neutron scattering. The experimental results and numerical analyses strongly suggest manifestation of highly frustrated quantum states in this cobaltite.

II. EXPERIMENTS

Initial single-crystal studies were performed at the NIST Center for Neutron Research using the BT-2 and BT-9 triple axis spectrometers. Single-crystal inelastic neutron scattering experiments were performed on the triple axis spectrometer TOPAN, installed at the JRR-3 reactor, Japan Atomic Energy Agency, Tokai, Japan. The final energy of the neutrons was fixed at $E_f = 13.5$ meV with horizontal collimation sequence of blank-100'-100'-blank. A sapphire filter and a pyrolytic graphite filter efficiently eliminated fast neutrons and the higher-order contamination, respectively. Single-crystal rods

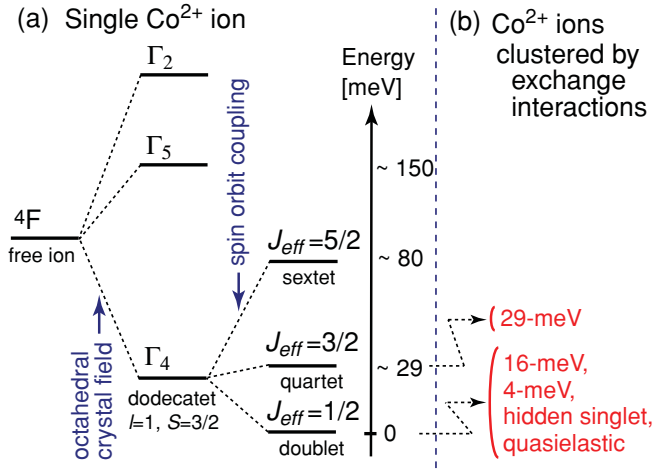


FIG. 1. (Color online) (a) Energy level scheme of Co^{2+} ion under octahedral crystal field and SOC. (b) Correspondence with the data measured in the present experiments.

of GeCo_2O_4 were grown by a floating zone method. Details of the crystal growth are summarized in Ref. 27. The rod size was about 4 mm in diameter and 30 mm high. The three co-aligned single crystals were enclosed with He exchange gas in an aluminum container, which was placed under the cold head of a closed-cycle He refrigerator.

Powder inelastic neutron scattering experiments were performed on the direct geometry chopper spectrometer HET, installed at the spallation neutron source, ISIS Facility, UK. The energy of the incident neutrons was fixed at $E_i = 59$ and 29 meV. A 35-g powder specimen of GeCo_2O_4 was synthesized by a solid-state reaction method, filled in an envelope made from thin aluminum foil, and inserted into a refrigerator with He exchange gas.

III. RESULTS

Figures 2(a) and 2(b) show the powder data with $E_i = 29$ meV. Above T_N the quasielastic mode is observed around $Q \equiv |\mathbf{Q}| = |\mathbf{q}_m| = 0.66 \text{ \AA}^{-1}$, as shown in Fig. 2(a). Below T_N spin-wave-like dispersion rises up from around $Q = |\mathbf{q}_m|$ in

addition to the previously discovered 4-meV mode,²¹ as shown in Fig. 2(b). Figures 2(c) and 2(d) show the data with $E_i = 59$ meV. Two discrete levels are discovered around $E = 16$ and 29 meV, both above and below T_N , indicating that the two modes are not spin waves. Below T_N these modes slightly sharpen and harden.

We measured Q correlations of the quasielastic mode above T_N and the 4-, 16-, and 29-meV modes below T_N in a constant- E scan mode by single-crystal inelastic neutron scattering, as shown in Figs. 3(a)–3(h). The scattering intensity distributions with characteristic patterns decrease at higher Q , as expected for the Co magnetic form factor, indicating that the excitations must be attributed to a magnetic origin and not a phononic one. Figures 3(a) and 3(b) show the data for the quasielastic mode, measured at $E = 4$ meV. The intensity is strong only in the 400, 440, and 222 Brillouin zones, and is distributed near the edges of the zones. Figures 3(c) and 3(d) show the data measured at 4 meV below T_N . Though it is difficult to remove the spin-wave component spread around $h/2 k/2 l/2$ reciprocal lattice points (magnetic Bragg reflection points for elastic scattering), the scattering pattern is quite similar to that for the quasielastic scattering. Figures 3(e)–3(h) show the data for the 16- and 29-meV modes. The scattering intensity of the former mode is relatively strong except for the above Brillouin zones, whereas that of the latter mode is distributed on every zone boundary.

IV. MODEL IDENTIFICATION

A. Quasielastic mode

We analyzed the quasielastic mode using a molecular model, as for the spin-frustrated systems.^{5,10} For elastic and quasielastic magnetic neutron scattering, the cross section is described by

$$S(\mathbf{Q}) = C_0 |F(\mathbf{Q})|^2 \left[\sum_{j=1}^N J_{j\perp} \exp(i\mathbf{Q} \cdot \mathbf{r}_j) \right]^2, \quad (1)$$

where C_0 is a proportional constant of intensity, $F(\mathbf{Q})$ is the magnetic form factor of the Co^{2+} ion, for which the Watson-Freeman one was used below,²⁸ j labels the site of the Co^{2+} , N

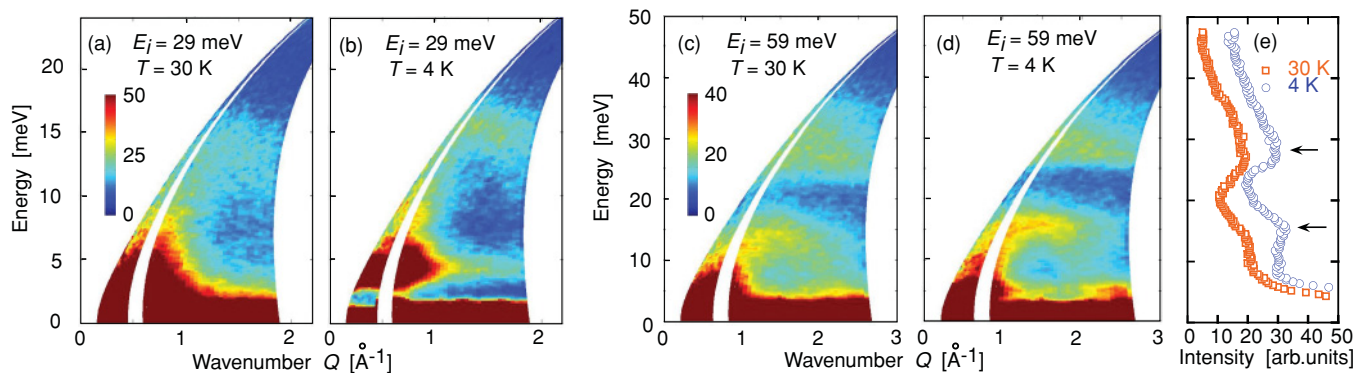


FIG. 2. (Color online) (a)–(d) Color images of powder inelastic neutron scattering data with different incident energies and temperatures. The color tones indicate the scattering intensity in $\text{mb}/(\text{sr}\cdot\text{formula})$ units. (e) Energy spectra, averaged from 3° to 29° in scattering angle ($Q = 0.3\text{--}2.7 \text{ \AA}^{-1}$ for elastic condition) in (c) and (d). The arrows indicate the 16- and 29-meV modes.

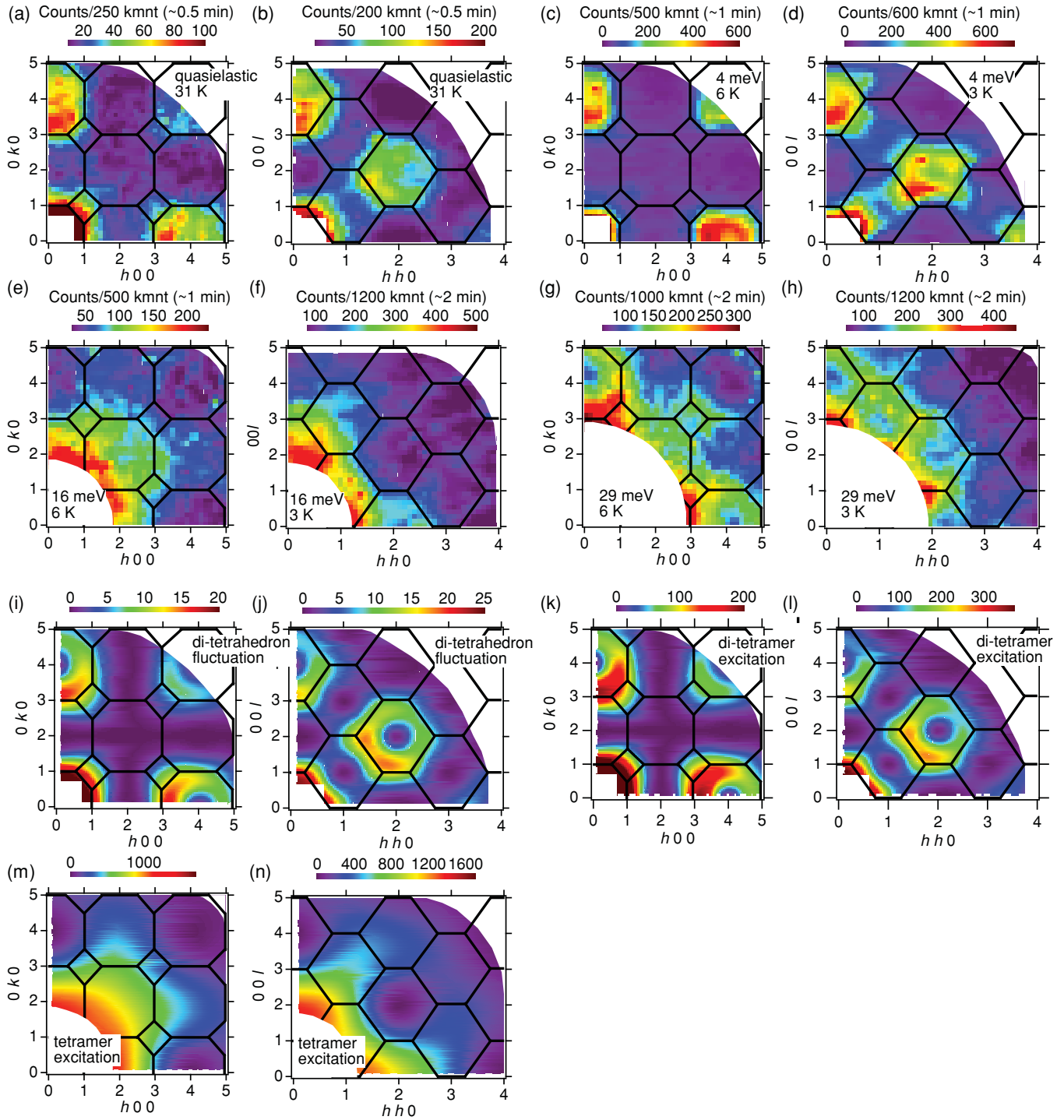


FIG. 3. (Color online) (a)–(h) Color images of single-crystal inelastic neutron scattering data, measured in the $hk0$ and hhl zones in a constant energy scan mode. (a) and (b) were measured at $E = 4$ meV. (i)–(n) One-to-one correspondence between calculated patterns as identified by the molecular models shown in Figs. 4(a)–4(f) and described in the text. The bold lines show the Brillouin zone boundary of the spinel structure. For the calculated patterns, the horizontal bars indicate the scattering intensity in arbitrary units. The abbreviation kmnt means 10^3 monitor counts of incident neutrons.

is the total number of sites in a molecule, \mathbf{r}_j and $\mathbf{r}_{j'}$ are those positions, and $J_{j\perp}$ is an expected value of the \mathbf{Q} -perpendicular component in \mathbf{J}_j .²⁹ When collinear \mathbf{J} 's fluctuate in arbitrary directions like in a hexagonal-type quasielastic mode observed in the typical spin-frustrated system ZnCr_2O_4 , $J_{j\perp}$ ($= S_{j\perp}$) takes on only ± 1 .⁵ The large square brackets indicate an

orientational average over equivalent molecules. Following this treatment, we searched for and found a di-tetrahedral model for the quasielastic mode in GeCo_2O_4 , as shown in Fig. 4(a). Figures 3(i) and 3(j) show the calculated patterns, which are in good agreement with the experimental patterns of Figs. 3(a) and 3(b).

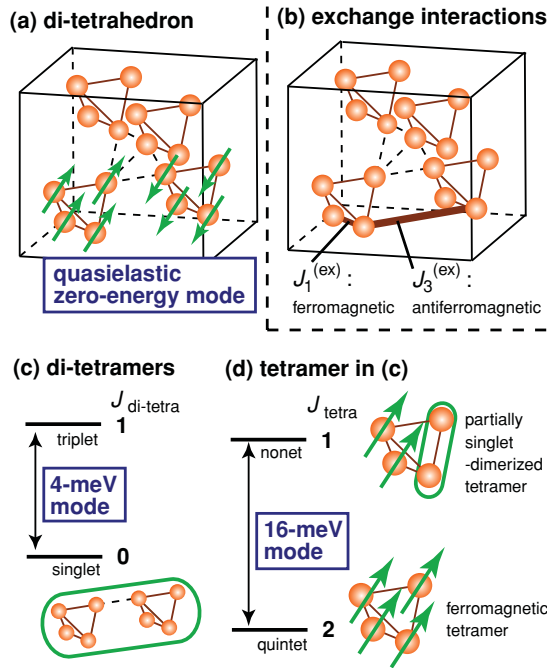


FIG. 4. (Color online) (a)(c)(d) Schematic representations of the molecular models. The green arrows represent magnetic moments of the Co^{2+} ion, and green ellipsoids represent a nonmagnetic singlet formation. All the moments dynamically fluctuate in arbitrary directions with the relative correlations. The structural units shown in (a) and (c) are identical to each other. In (c), the representative states are depicted. (b) First- and third-neighbor exchange interactions. Representative bonds are shown.

B. 4- and 16-meV modes

For inelastic magnetic neutron scattering, the cross section is described by

$$S(\mathbf{Q}, E) = C_0 |F(\mathbf{Q})|^2 \delta(\hbar\omega - E) \left[\sum_{\alpha, \beta=1}^3 \left(\delta_{\alpha\beta} - \frac{Q_\alpha Q_\beta}{|\mathbf{Q}|^2} \right) \times \sum_{j, j'=1}^N \langle \lambda | \hat{J}_j^\alpha | \lambda' \rangle \langle \lambda' | \hat{J}_{j'}^\beta | \lambda \rangle \exp\{i \mathbf{Q} \cdot (\mathbf{r}_j - \mathbf{r}_{j'})\} \right], \quad (2)$$

where α and β are (x, y, z) , N is number of sites in a molecule, $|\lambda\rangle$ and $|\lambda'\rangle$ are molecular ground and excited states, respectively, \hat{J} is a total angular momentum operator, and the large square brackets indicate an orientational average over equivalent molecules.²⁹ One cannot generally apply Eq. (1), which is obtained from Eq. (2) only when the matrix elements $\langle \lambda' | \hat{J}_j^\alpha | \lambda \rangle$ can be simply reduced for elastic scattering. In the following we try to reproduce our inelastic scattering data using a relatively simple molecular model. We assume effective molecular Hamiltonians, and numerically evaluate $\langle \lambda' | \hat{J}_j^\alpha | \lambda \rangle$ and the cross section. The assumption of a molecular formation implies a remarkably mixed molecular orbital, which will enhance intramolecular exchange interactions and suppress atomic orbital characters like anisotropy.³⁰ Therefore, we ignore the exchange field outside the molecule (Lorentz-

like local magnetic field) and the directional term $(\delta_{\alpha\beta} - Q_\alpha Q_\beta / |\mathbf{Q}|^2)$ in Eq. (2). An orientational average over dynamically fluctuating molecules will also substantially suppress the directional dependence. For simplicity the atomic Watson-Freeman form factor is used for $F(\mathbf{Q})$ in Eq. (2) again.²⁸

First, we exactly diagonalized a tetramer Hamiltonian:

$$\hat{H}_{\text{tetra}} = J_1^{(\text{ex})} \sum_{i,j=1}^4 \hat{J}_i \cdot \hat{J}_j, \quad (3)$$

where $J_i = 1/2$, i and j are positions of the tetrahedral sites [Fig. 4(d)], $\sum_{i,j}$ means summation over all J pairs (not doubly counted), and $J_1^{(\text{ex})}$ is a first-neighbor exchange interaction that is ferromagnetic as expected from the quasielastic mode [Fig. 4(a)] and the Goodenough-Kanamori rule.³¹ The 16 ($= 2^4$) basis states of $|J_1^z, J_2^z, J_3^z, J_4^z\rangle$ were used, where $J_i^z = \pm 1/2$. Figure 4(d) shows the obtained level scheme with $J_1^{(\text{ex})} = -8$ meV. The ground states are described as ferromagnetic quintets with $J_{\text{tetra}} = 2$, and the first excited states are nonets with $J_{\text{tetra}} = 1$ and $E = 16$ meV, where $J_{\text{tetra}} = \sum_{i=1}^4 J_i$. The nonet can generate all states with $J_{\text{tetra}}^z = \pm 1, 0$ with a $J_{\text{eff}} = 1/2$ dimer-singlet bond by their linear combinations [e.g., Fig. 4(d)]. The calculated patterns for excitation processes from the ground states to the excited states are shown in Figs. 3(m) and 3(n), which are in excellent agreement with the experimental patterns of Figs. 3(e) and 3(f) (16 meV).

Second, we diagonalized a di-tetramer Hamiltonian

$$\hat{H}_{\text{di-tetra}} = J_{ij}^{(\text{ex})} \sum_{i,j=1}^8 \hat{J}_i \cdot \hat{J}_j, \quad (4)$$

where $J_{ij}^{(\text{ex})} = J_1^{(\text{ex})}$ and $J_3^{(\text{ex})}$, i and j are positions of sites in the di-tetramer [Fig. 4(c)], and the 256 ($= 2^8$) basis states of $|J_1^z, J_2^z, J_3^z, \dots, J_8^z\rangle$ were used. The sign of $J_3^{(\text{ex})}$ is antiferromagnetic, being consistent with the quasielastic mode and previous neutron diffraction reports.²⁵ Figure 4(c) shows the level scheme with $J_1^{(\text{ex})} = -8$ meV and $J_3^{(\text{ex})} = 10$ meV. The ground state is described as a nonmagnetic singlet with $J_{\text{di-tetra}} = 0$, and the first excited states are triplet with $J_{\text{di-tetra}} = 1$, where $J_{\text{di-tetra}} = \sum_{i=1}^8 J_i$. Figures 3(k) and 3(l) show the calculated patterns of the singlet-triplet excitations, which are similar to those for the quasielastic mode [Figs. 3(i) and 3(j)], and are identified as the 4-meV mode.

Equations (3) and (4) gave many other excited eigenstates with higher energies; e.g., in Eq. (3), a second excited $J_{\text{tetra}} = 0$ doublet with 24 meV (the highest-energy mode), and in Eq. (4), a second excited $J_{\text{di-tetra}} = 2$ quintet with 10 meV, a third excited $J_{\text{di-tetra}} = 3$ septet with 17 meV, fourth, fifth, and sixth excited $J_{\text{di-tetra}} = 1$ triplets with 18, 21, and 22 meV, respectively, and so on. Intensities of the 24-, 10-, and 17-meV multiplets were estimated to be zero, and are not observed in the present experiments as well. Intensities of the 18-, 21-, and 22-meV triplets were estimated to be less than 5% of those of the first excited 4-meV triplet, and are also not clearly recognized in the experimental energy spectrum [Fig. 2(e)].

We could not simultaneously reproduce the 4- and 16-meV modes within Eq. (4). This fact is unlike normal molecular magnets, in which a single equation (Hamiltonian) governs

all the excitations. The one interpretation might be that the two modes arise from different domains. The domains might be static, or possibly fluctuate slowly. We remark that slow spin fluctuations with $\sim 10^{-5}$ s are observed even at temperatures of \sim mK order in representative frustrated spinel materials MgCr_2O_4 ($T_N = 13$ K) and CdCr_2O_4 by muon spin resonance.³² The other interpretation might be that the complete Hamiltonian is much more complex; e.g., it cannot be simply described by only \mathbf{J} but also by the lattice and charge degrees of freedom. Such couplings among multiple degrees of freedom are often enhanced to suppress frustration.^{33,34} The two interpretations cannot be distinguished at this stage, which will require further theoretical and experimental studies in future.

C. 29-meV mode

For the 29-meV mode, we could find no model within $J_i = 1/2$ after many trials. On the other hand, interestingly, other cobalt compounds KCoF_3 , CoO , and $\text{La}(\text{Sr})_2\text{CoO}_4$, consisting of Co^{2+} ions octahedrally surrounded by anions as well, exhibit excitations around 30 meV.^{35–38} These excitations are interpreted as the lowest-energy SOC excitations (i.e., excitons).^{35–38} In analogy with these cobalt compounds, the 29-meV mode in GeCo_2O_4 is to be excitons.

The \mathbf{Q} patterns along the Brillouin zone boundary [Figs. 3(g) and 3(h)] demonstrate that the excitons exhibit spatial correlations. Further, the correlations are qualitatively estimated as follows. The Brillouin zone boundary of the spinel structure corresponds to third-neighbor antiferromagnetic correlations in connection with the inverse of the Q values within Eq. (1). There are expected to be few first-neighbor ferromagnetic correlations, since such correlations give rise to extinction rules in structure factors, as shown in Figs. 3(i) and 3(j) for the di-tetrahedron model. Meanwhile, the structure-factor part in Eq. (1) is proportional to $\sum_{j,j'=1}^N J_{j\perp} J_{j'\perp} \exp[i\mathbf{Q} \cdot (\mathbf{r}_j - \mathbf{r}_{j'})]$, which is common with the part in Eq. (2) in the sense of the correlation function between two sites j and j' , though it cannot be distinguished whether the excited states are antiferromagnetic or ferromagnetic. Thus, the \mathbf{Q} patterns of the 29-meV mode strongly suggest third-neighbor correlations even for inelastic scattering as well.

In this way, the 29-meV mode can be understood as the processes that the intermultiplet excitation from $J_{\text{eff}} = 1/2$ to $3/2$ appearing at a single Co^{2+} site dissipates to the third-neighbor sites. It is notable that the intermultiplet excitations appreciably exhibit spatial correlations, since they are normally regarded as single-site excitations.^{39,40} It is also interesting that first-neighbor correlations are not dominant, which is probably because orbital mixing (therefore exchange interactions) between a $J = 3/2$ site and a $J = 1/2$ site in the excited states is different from that between two $J = 1/2$ sites.

The experimental spectrum around 29 meV is asymmetrically spread up to 40 meV, as shown in Fig. 2(e). More precisely, the Co^{2+} feels an additional trigonal component of crystal electric field, which keeps the $J_{\text{eff}} = 1/2$ ground doublet but splits the $J_{\text{eff}} = 3/2$ quartet into two Kramers doublets ($J_{\text{eff}}^z = \pm 3/2$ doublet and $J_{\text{eff}}^z = \pm 1/2$ one) in the level scheme shown in Fig. 1(a).^{20,21} Therefore, the spreading of the spectrum will be due to the splitting of the $J_{\text{eff}} = 3/2$ quartet.

The remaining Γ_4 states described by $J_{\text{eff}} = 5/2$ are estimated to be distributed around 80 meV, since the ratio of SOC energy of $J_{\text{eff}} = 5/2$ sextet to that of $J_{\text{eff}} = 3/2$ quartet is theoretically calculated to be $8/3$.¹⁹ The excitation processes from the $J_{\text{eff}} = 1/2$ to the $J_{\text{eff}} = 5/2$ are forbidden owing to the angular-momentum conservation law, which allows only the angular-momentum transitions of ± 1 and 0 in the dipole approximation with strong scattering intensity.²⁹ In fact, there is no report of magnetic excitations around this energy by inelastic neutron scattering.^{21,41} On the other hand, magnetic excitations were observed around 150 meV,^{21,41} which will come from the Γ_5 states shown in Fig. 1(a) (octahedral crystal field excitations).

D. Summary of identification

We identified the quasielastic mode as an antiferromagnetic di-tetrahedral cluster [Fig. 4(a)], consisting of Co^{2+} ions with $J_{\text{eff}} = 1/2$. Furthermore, we assigned the 4-meV to the singlet-triplet excitations in a di-tetramer with the same structural unit [Fig. 4(c)], the 16-meV to quintet-nonet excitations in the one ferromagnetic tetramer [Fig. 4(d)], and the 29-meV to SOC excitons from $J_{\text{eff}} = 1/2$ to $3/2$ with third-neighbor correlations. The correspondence relations between excitations and J_{eff} states are shown in Fig. 1(b).

V. DISCUSSION

We discuss the ferromagnetic tetramer units appearing both in the 4- and 16-meV modes. The remarkable spatial confinement of magnetic correlation demonstrates the existence of frustration. But frustration is normally based on antiferromagnetism. So what is frustrated in GeCo_2O_4 ? One factor will be the spin-ice frustration, since the Co^{2+} moment would have been Ising-like unless the tetramer formation occurred,³⁰ and since the spin-ice frustration is generated by ferromagnetic $J_1^{(\text{ex})}$ as shown in f -electron pyrochlore systems.⁷ The tetramer formation seems to be characteristic of d -electron spin-ice frustration with relatively strong exchange interactions. Another factor will be the frustration among exchange interactions $J_1^{(\text{ex})}$, $J_3^{(\text{ex})}$, and so on. The other factor will be orbital frustration that an orbital system is inherently frustrated even on a simple cubic lattice; when orbitals (directions of the electron cloud) are arranged to gain bond energy for one direction, this configuration is not fully favorable for other bonds.^{42–44} GeCo_2O_4 also has an orbital angular momentum, which is a kind of orbital, and is in the geometrically frustrated pyrochlore lattice. Therefore, spin-ice, exchange, and orbital frustration likely coexist in GeCo_2O_4 .

Next we discuss the di-tetramer. According to the above analyses, the di-tetramer singlet ground state is surprisingly hidden as origin of the molecular excitations below T_N . Indeed, a singlet formation is an effective way to suppress frustration and degree of freedom. However, the formation does not necessarily mean that all the magnetic moment disappears, because the g factor is arbitrary in our analyses, being consistent with the coexistence of singlet and magnetic order. This partial-singlet model can explain why GeCo_2O_4 exhibits magnetic order with only about $3 \mu_B$ per Co^{2+} ,⁴⁵ which is $1 \mu_B$ lower than a normal value of $4 \mu_B$ generated by SOC as in CoO .¹⁹

It should be noted that a typical spin-frustrated spinel antiferromagnet MgCr_2O_4 (Cr^{3+} , d^3 , $S = 3/2$) similarly exhibits a set of quasielastic modes above T_N (hexamer) and a gapped nondispersive excitation mode below T_N , of which the scattering intensity distributions in \mathbf{Q} space are the same.¹⁰ In addition, MgCr_2O_4 exhibits magnetic order with only $2.2 \mu_B$,⁴⁶ which is about $1 \mu_B$ lower than the full moment $3 \mu_B$. Therefore, a hexamer-type singlet ground state would give rise to both the gapped excitation mode and the partial disappearance of the magnetic moment below T_N . We also remark that the $1 \mu_B$ decrease is observed in the isomorphic systems ZnCr_2O_4 and HgCr_2O_4 .^{47,48}

The di-tetramer can be energetically regarded as a dimer of the rigid tetramers with $J_{\text{tetra}} = 2$; binding energy in a ferromagnetic tetramer [$\sim 36 \text{ meV} = 6J_1^{(\text{ex})}J_{\text{eff}}(J_{\text{eff}} + 1)$] is higher than antiferromagnetic coupling energy between the two tetramers [$\sim 24 \text{ meV} = (4J_3^{(\text{ex})} + J_1^{(\text{ex})})J_{\text{eff}}(J_{\text{eff}} + 1)$]. We also numerically confirmed that the $J_{\text{tetra}}=2$ dimer has a ground singlet with the combination of $J_{\text{tetra},i}^z = \pm 2, \pm 1, 0$ and the first excited triplets within the 25 ($= 5^2$) basis states of $|J_{\text{tetra},1}^z, J_{\text{tetra},2}^z\rangle$, and also confirmed that the singlet-triplet excitations of the $J_{\text{tetra}}=2$ dimer show the same \mathbf{Q} patterns as those for the di-tetramer. This extended-dimer picture naturally gives us the interpretations of the 4-meV mode as a localized singlet-triplet excitation and of the quasielastic mode as its precursor fluctuations, as observed in the frustrated spin-1/2 system $\text{SrCu}_2(\text{BO}_3)_2$ with the two-dimensional Shastry-Sutherland lattice.⁴⁹

Since its introduction as a mechanism for high-temperature superconductivity, dimer-based quantum cooperative phenomena such as resonating valence bond (RVB) and valence bond solid (VBS) have been sought in fields of magnetism and strongly correlated electron systems.⁵⁰ $\text{SrCu}_2(\text{BO}_3)_2$ is one of the great successes. In contrast to the borate, the molecular formations in GeCo_2O_4 are characterized by the existence of a ferromagnetic molecule, $J_{\text{eff}} = 1/2$, and the three-dimensional pyrochlore lattice with almost regular triangles. In this sense, GeCo_2O_4 could be positioned as a new class of quantum cooperative systems caused by frustration and $J_{\text{eff}} = 1/2$.

We list two other intriguing characters of frustration and $J_{\text{eff}} = 1/2$. One character is that all the molecular excitations

involve aspects of not only spin but also orbital excitations by SOC (molecular orbitons). Another character is the emergence of very diffusive excitons (29 meV). Excitons normally appear within a single atom or ion with SOC, and are occasionally propagated with very narrow dispersion width ($\sim 0.5 \text{ meV}$) as in a $4f$ electron system.⁵¹ Furthermore, the $3d$ electron cobalt systems exhibit more dispersive excitons around 30 meV (over 5 meV width), propagated by stronger exchange interactions than in $4f$ systems.^{35–38} However, these excitons are locally collective but are not propagated.

VI. CONCLUSIONS

We discovered several types of nondispersive short-range excitations in a three-dimensional frustrated GeCo_2O_4 with $J_{\text{eff}} = 1/2$ by powder and single-crystal inelastic neutron scattering. The scattering intensity maps in \mathbf{Q} space are well reproduced by quantum-mechanical molecular models. The model analyses suggest that the molecular excitations below T_N arise from molecular ground states, one of which consists of antiferromagnetically coupled ferromagnetic subunits. The quasielastic excitations above T_N are interpreted as a precursor of this quantum ground state. The spin and orbital frustration of J_{eff} lead to the molecular-singlet formation and the ferromagnetic molecule one, respectively. Further experimental and theoretical works will be needed to fully elucidate this hidden molecular partial-singlet conjecture and clarify the molecular orbital formations.

ACKNOWLEDGMENTS

We thank Mr. M. Ohkawara, Mr. K. Nemoto and Mr. T. Asami for their support in JAEA, Mr. M. Onodera for his support in Tohoku University, and Professors Y. Motome and S. Ishihara for fruitful discussions. The neutron experiments in JAEA were performed under User Programs conducted by ISSP, University of Tokyo. This work was supported by the MEXT of Japan, Grants in Aid Young Scientists (B) (22740209), Priority Areas (22014001), Scientific Researches (S) (21224008) and (A) (22244039) and Innovative Areas (20102005), and by Tohoku University, Inter-university Cooperative Research Program of the Institute for Materials Research.

*tomiyasu@m.tohoku.ac.jp

¹L. Pauling, *J. Am. Chem. Soc.* **57**, 2680 (1935).

²G. H. Wannier, *Phys. Rev.* **79**, 357 (1950).

³P. W. Anderson, *Phys. Rev.* **102**, 1008 (1956).

⁴R. Ballou, E. Lelievre-Berna, and B. Fåk, *Phys. Rev. Lett.* **76**, 2125 (1996).

⁵S.-H. Lee, C. Broholm, W. Ratcliff, G. Gasparovic, Q. Huang, T. H. Kim, and S.-W. Cheong, *Nature (London)* **418**, 856 (2002).

⁶Y. Yasui, M. Kanada, M. Ito, H. Harashina, M. Sato, H. Okumura, K. Kakurai, and H. Kadowaki, *J. Phys. Soc. Jpn.* **71**, 599 (2002).

⁷S. T. Bramwell and M. J. P. Gingras, *Science* **294**, 1495 (2001).

⁸S. Nakatsuji, Y. Nambu, H. Tonomura, O. Sakai, S. Jonas, C. Broholm, H. Tsunetsugu, Y. Qiu, and Y. Maeno, *Science* **309**, 1697 (2005).

⁹H. Kawamura, A. Yamamoto, and T. Okubo, *J. Phys. Soc. Jpn.* **79**, 023701 (2010).

¹⁰K. Tomiyasu, H. Suzuki, M. Toki, S. Itoh, M. Matsuura, N. Aso, and K. Yamada, *Phys. Rev. Lett.* **101**, 177401 (2008).

¹¹B. J. Kim *et al.*, *Phys. Rev. Lett.* **101**, 076402 (2008).

¹²B. J. Kim, H. Ohsumi, T. Komesu, S. Sakai, T. Morita, H. Takagi, and T. Arima, *Science* **323**, 1329 (2009).

¹³A. Shitade, H. Katsura, J. Kunes, X.-L. Qi, S.-C. Zhang, and N. Nagaosa, *Phys. Rev. Lett.* **102**, 256403 (2009).

¹⁴J. W. Lynn, G. Shirane, and M. Blume, *Phys. Rev. Lett.* **37**, 154 (1976).

¹⁵Y. Okamoto, M. Nohara, H. Aruga-Katori, and H. Takagi, *Phys. Rev. Lett.* **99**, 137207 (2007).

- ¹⁶K. Matsuhira, M. Wakeshima, R. Nakanishi, A. N. T. Yamada, W. Kawano, S. Takagi, and Y. Hinatsu, *J. Phys. Soc. Jpn.* **76**, 043706 (2007).
- ¹⁷M. Sakata, T. Kagayama, K. Shimizu, K. Matsuhira, S. Takagi, M. Wakeshima, and Y. Hinatsu, *Phys. Rev. B* **83**, 041102(R) (2011).
- ¹⁸Neutron News **3**, 29 (1992).
- ¹⁹J. Kanamori, *Prog. Theor. Phys.* **17**, 177 (1957).
- ²⁰M. E. Lines, *Phys. Rev.* **131**, 546 (1963).
- ²¹J. C. Lashley, R. Stevens, M. K. Crawford, J. Boerio-Goates, B. F. Woodfield, Y. Qiu, J. W. Lynn, P. A. Goddard, and R. A. Fisher, *Phys. Rev. B* **78**, 104406 (2008).
- ²²T. Watanabe, S. Hara, and S. I. Ikeda, *Phys. Rev. B* **78**, 094420 (2008).
- ²³J. Hubsch and G. Gavoille, *J. Magn. Magn. Mater.* **66**, 17 (1987).
- ²⁴S. Diaz, S. de Brion, M. Holzapfel, G. Chouteau, and P. Strobel, *Physica B* **346**, 146 (2004).
- ²⁵S. Diaz, S. de Brion, G. Chouteau, B. Canals, V. Simonet, and P. Strobel, *Phys. Rev. B* **74**, 092404 (2006).
- ²⁶T. Hoshi, H. A. Katori, M. Kosaka, and H. Takagi, *J. Magn. Magn. Mater.* **310**, e448 (2007).
- ²⁷S. Hara, Y. Yoshida, S. I. Ikeda, N. Shirakawa, M. K. Crawford, K. Takase, Y. Takano, and K. Sekizawa, *J. Cryst. Growth* **283**, 185 (2005).
- ²⁸R. E. Watson and A. J. Freeman, *Acta Crystallogr.* **14**, 27 (1961).
- ²⁹W. Marshall and S. W. Lovesey, *Theory of Thermal Neutron Scattering* (Oxford University, Oxford, 1971).
- ³⁰In an atomic orbital approximation, the quantization z axis of Co^{2+} ions will be parallel to the $\langle 111 \rangle$ direction like spin ice.²¹
- ³¹J. B. Goodenough, *Phys. Rev.* **117**, 1442 (1960).
- ³²M. T. Rovers, P. P. Kyriakou, H. A. Dabkowska, G. M. Luke, M. I. Larkin, and A. T. Savici, *Phys. Rev. B* **66**, 174434 (2002).
- ³³K. Matsuda, N. Furukawa, and Y. Motome, *J. Phys. Soc. Jpn.* **75**, 124716 (2006).
- ³⁴Y. Motome, K. Penc, and N. Shannon, *J. Magn. Magn. Mater.* **300**, 57 (2006).
- ³⁵T. M. Holden, W. J. L. Buyers, E. C. Svensson, R. A. Cowley, M. T. Hutchings, D. Hukin, and R. W. H. Stevenson, *J. Phys. C* **4**, 2127 (1971).
- ³⁶W. J. L. Buyers, T. M. Holden, E. C. Svensson, R. A. Cowley, and M. T. Hutchings, *J. Phys. C* **4**, 2139 (1971).
- ³⁷K. Tomiyasu and S. Itoh, *J. Phys. Soc. Jpn.* **75**, 074808 (2006).
- ³⁸L. M. Helme, A. T. Boothroyd, R. Coldea, D. Prabhakaran, C. D. Frost, D. A. Keen, L. P. Regnault, P. G. Freeman, M. Enderle, and J. Kulda, *Phys. Rev. B* **80**, 134414 (2009).
- ³⁹E. Balcar and S. W. Lovesey, *J. Phys. C* **19**, 4605 (1986).
- ⁴⁰W. G. Williams, B. C. Boland, Z. A. Bowden, A. D. Taylor, S. Culverhouse, and B. D. Rainford, *J. Phys. F* **17**, L151 (1987).
- ⁴¹M. K. Crawford *et al.* (unpublished).
- ⁴²D. I. Khomskii and M. V. Mostovoy, *J. Phys. A* **36**, 9197 (2003).
- ⁴³T. Tanaka and S. Ishihara, *Phys. Rev. Lett.* **98**, 256402 (2007).
- ⁴⁴J. Nasu, A. Nagano, M. Naka, and S. Ishihara, *Phys. Rev. B* **78**, 024416 (2008).
- ⁴⁵M. Matsuda, T. Hoshi, H. Aruga-Katori, M. Kosaka, and H. Takagi, *J. Phys. Soc. Jpn.* **80**, 034708 (2011).
- ⁴⁶H. Shaked, J. M. Hastings, and L. M. Corliss, *Phys. Rev. B* **1**, 3116 (1970).
- ⁴⁷S. Ji, S.-H. Lee, C. Broholm, T. Y. Koo, W. Ratcliff, S.-W. Cheong, and P. Zschack, *Phys. Rev. Lett.* **103**, 037201 (2009).
- ⁴⁸M. Matsuda, H. Ueda, A. Kikkawa, Y. Tanaka, K. Katsumata, Y. Narumi, T. Inami, Y. Ueda, and S.-H. Lee, *Nature Phys.* **3**, 397 (2007).
- ⁴⁹H. Kageyama, M. Nishi, N. Aso, K. Onizuka, T. Yoshihama, K. Nukui, K. Kodama, K. Kakurai, and Y. Ueda, *Phys. Rev. Lett.* **84**, 5876 (2000).
- ⁵⁰P. W. Anderson, *Science* **235**, 1196 (1987).
- ⁵¹K. Kuwahara *et al.*, *Phys. Rev. Lett.* **95**, 107003 (2005).